17th Brazilian Congress of Thermal Sciences and Engineering
November 25th-28th, 2018, Águas de Lindóia, SP, Brazil

ENCIT-2018-0547
UNCERTAINTY ANALYSIS OF TRANSIENT PROBLEMS USING MONTE CARLO METHOD

Hiago Souza da Silva
Tainan Gabardo Miranda dos Santos
Federal University of Technology – Parana, Rua Deputado Heitor Alencar Furtado, 5000, Curitiba, PR.
hiago@alunos.utfpr.edu.br
tainansantos@utfpr.edu.br

Cezar Otaviano Ribeiro Negrão
Federal University of Technology – Parana, Rua Deputado Heitor Alencar Furtado, 5000, Curitiba.
negrao@utfpr.edu.br

Abstract.
Uncertainties in mathematical models appears due to lack of knowledge of the physical phenomena being described and its intrinsic randomness. A proper quantification makes the model more robust and feasible. For processes involving safety and reliability, an assessment of the effects of uncertainties is crucial in order to prevent and avoid catastrophic failures and undesirable events. This study investigates the pressure needed to restart the flow during the drilling process. The problem is considered as a pipeline filled with gelled drilling fluid at rest. In order to start up the flow, a pressure higher than the usual is required. It is essential to control the pressures involved in the process as a higher pressure may damage the formation and a lower pressure may cause a kick. The damage on the formation represents a loss of drilling fluid to the formation and the kick may cause serious problems such as a blowout. These problems can cause environmental and financial issues. In order to assure that the pressure is between this narrow gap, it is necessary to model the uncertainties associated to the restart problem. The objective of this paper is to use the Monte Carlo Method to assess the uncertainties during flow start-up conditions.

Keywords: *restart, Monte Carlo Method, LHS, mathematical model, transient simulation*

1. INTRODUCTION

Crude oil is one of the most demanded commodities, due to its vast use in the industries of plastics, fuels, among others (Morais 2013). Once the onshore reservoirs are becoming scarcer, the offshore production received some relevance and visibility, since it was already found large amounts of oil, especially in the Brazilian coast.

Offshore oil production is achieved by using a rotating bit, equipped with a drilling column. The rotation movement of the drill and the weight of the column are the means to drill the well. The drilling process generates gravel, which may block the movement of the drill (Thomas 2001). In order to avoid it, drilling mud is employed. The main function of this drilling fluid is to drag the gravel away from the drill by carrying them through the annular space between the drill pipe and the wall of the well (Caenn et al. 2011). In order to fulfill its main function, the drilling fluid must have some interesting properties, such as forming a gel-like structure at rest, preventing the gravel from returning to the drill when the flow is stopped, and recovering its fluid state when the flow is restarted (Lummus and Azar 1986). In order to start-up the flow, pressures higher than the usual are necessary.

This pressure control must be carefully carried out due to the influence pressure has on the whole well. If the pressure is low, a phenomenon called kick may occur (Galves 2013), i.e. there may be a migration of fluid from the formation to the well. On the other hand, higher pressures may promote fractures in the rock formation, which can cause loss of drilling fluid to the formation (Santos 2006). Therefore, the pressure range is way too narrow and difficult to control, making this variable one of the most critical in the process.

In order to start-up the flow, an inlet flow rate or pressure must be applied. This sudden boundary condition characterizes the restart of the flow as a transient problem (Wylie et al. 1993). These kind of problems, due to its inherent time dependency, are difficult to model. Other transient problems normally studied are the fluid hammer (Streeter and Lai 1962; Bergant et al. 2006; Wahba 2006) and the pressure transmission (Oliveira et al. 2012; Oliveira et al. 2013).

Fluid hammer, a generalization of the water hammer, is characterized by the sudden closure of a valve in pipeline with fluid previously flowing. This fast closure causes a pressure peak in the pipeline and has been studied by many authors that modeled the fluid as Newtonian (Ghidaoui and Kolyshkin 2001; Zhao and Ghidaoui 2003; Ghidaoui et al. 2005) and non-Newtonian (Wahba 2013; Tazraei et al. 2015; Oliveira et al. 2015; Tazraei and Riasi 2015; Majd et al.

2016; Yang et al. 2017). Such as other transient problems, the assessment of the velocities and pressures involved in the phenomenon is still a challenging task.

The pressure transmission problem is observed in closed wells (Oliveira et al. 2012). During drilling operations some valves are closed due to pressure difference. The fluid is pumped into the well in order to transmit the pressure and operate the valve. Nevertheless, drilling engineers have reported that in viscoplastic fluids the pressure is not transmitted as expected (Oliveira et al. 2013). Therefore, the fluid has to be replaced by a Newtonian one. This is an expensive and time consuming solution.

Once these transient problems are normally related to safety and reliability, it is desirable to know with good precision how the parameters of the problem vary around their nominal values. This is essential because uncertainties on the models arise from the fluctuations in the parameters. Therefore, it is opportune to have a methodology to determine and quantify the uncertainties in the results of the model based in the uncertainties of the parameters.

Due to the complexity of the models employed in transient problems, it is unlikely, or even impossible, to derive analytical expressions for the uncertainties. A good way to overcome this inconvenient is to use statistical approaches. One of the most famous statistical methods to determine uncertainties is the Monte Carlo method, never seen before in the literature with this specific application.

In order to have the uncertainty quantification in the transient models, it is necessary to apply the concepts of the Monte Carlo into the traditional simulation, adapting them to assure viability of the whole calculus. Therefore, the objective of this paper is to develop an implementation of the Monte Carlo method applied to transient problems, assessing the convergence and fidelity of the results and its uncertainties.

2. MONTE CARLO METHOD

Over more than 60 years, the concepts and ideas around the name Monte Carlo found applications in all kinds of knowledge areas, such as physics, engineering, econometrics, game theory, among others. That was possible due to the approach of modelling uncontrolled (sometimes uncontrollable) variables or parameters as non-deterministic phenomena when their effects could not be neglected.

The concept of random-results phenomena is one of the motivations for using the probability theory, as an attempt of inferring deterministically features of non-deterministic situations, under reasonable assumptions. Two results of probability give some ground to work upon this way of modelling: the law of large numbers and the Central Limit Theorem. Relying on both, Metropolis and Ulam (1949) proposed the Monte Carlo method (MCM).

As stated by the Central Limit Theorem, any combinations (sums) of random variables is normally (gaussian) distributed (Triola 2017). This distribution is defined by two parameters: a mean value and a variance. Therefore, the Monte Carlo Method returns the mean value as its main result and the uncertainty is derived from the variance of the resultant random variable.

The Law of Large Numbers says that, when the number of experiments tends to infinity, the mean value of the sample tends to the theoretical expected value (Kalos and Whitlock 2008). This is applied in the Monte Carlo Simulation by solving the model several times, in order to assure that the mean of the sample and its uncertainties have converged.

The capabilities of the Monte Carlo method did not find application at first, since it required higher computational resources, not easily available at that time. Therefore, its implementations were a lot restricted. With the consolidation of electronic computing and the power brought by the evolution of transistors, the automation of iterative and repetitive calculations became popular, expanding the possibilities of use for Monte Carlo simulations (Bauer 1958). Therefore, it is possible to summarize the concept of the Monte Carlo Method as massive realizations (sampling) of random parameters. (Cunha et al. 2014).

Figure 1 exemplifies the idea of the method: a) the mathematical model is selected; b) the parameters are defined as random variables according to a chosen distribution (which can be defined by the following values: mean, standard deviation, degrees of freedom, skewness, etc.); c) the variables are sampled and applied to the model; d) the process is repeated a predefined number of times; and e) all the data previously acquired is processed to obtain the results along with its uncertainty.

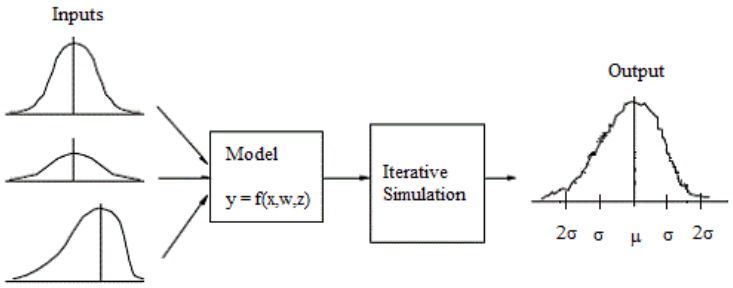

Figure 1. Scheme of the Monte Carlo Method. Adapted from: Martínez (2009)

2.1 Statistical definitions

For a good understanding of the how Monte Carlo method works, it is interesting to know some statistical concepts. Starting from random variable, which is a variable that has a single numerical value, determined by chance, for each outcome of a procedure. A probability distribution function (PDF) is a rule that defines the probability of occurrence for each value of the random variable (Triola 2017). The normal distribution and the uniform distribution are famous PDFs presented in Eq. (1) and Eq. (2), respectively. A useful version of the normal distribution, called standard normal distribution (Eq (3)), is defined when the mean is zero and the variance is unitary.

$$f(x) = \frac{1}{\sqrt{2\pi\sigma^2}} \exp\left[-\frac{(x-\mu)^2}{2\sigma^2} \right] \tag{1}$$

$$f(x) = \begin{cases} \dfrac{1}{a-b}, & if \quad a < x < b \\ 0, & \text{otherwise} \end{cases} \tag{2}$$

$$f(x) = \frac{1}{\sqrt{2\pi}} \exp\left[-\frac{x^2}{2} \right] \tag{3}$$

where μ stands for the mean, σ is the standard deviation (σ^2 is defined as the variance), and a, b are the upper and lower limit values, respectively.

Similarly to the PDF, the Cumulative Distribution Function (CDF) defines the probability of a random variable X return a value equal or smaller than a certain value x, belonging to the domain of X (Rubinstein 1991). The CDF of the normal distribution, uniform distribution and standard normal distribution are presented in Eq. (4), Eq. (5) and Eq. (6) respectively.

$$F(x) = \frac{1}{2}\left\{ 1 - \frac{2}{\sqrt{\pi}} \int_0^x \exp\left[-\left(\frac{y-\mu}{\sqrt{2\sigma^2}} \right)^2 \right] dy \right\} \tag{4}$$

$$F(x) = \begin{cases} 0, & if \; x < a \\ \dfrac{x-a}{b-a}, & if \; a < x < b \\ 1, & if \; x > b \end{cases} \tag{5}$$

$$F(x) = \frac{1}{2}\left\{ 1 - \frac{2}{\sqrt{\pi}} \int_0^x \exp\left[-y^2 \right] dy \right\} \tag{6}$$

The inverse of the CDF, popularly called Quantile function, converts a probability domain (between 0 and 1) into the domain of the random variable. Since this function does not have an analytical solution, in this paper an approximation proposed by Beasley et al. (2003) will be employed.

Another prerequisite for a successful Monte Carlo simulation is a good method of generation for the realizations of the random variables. This is done by using pseudo-random numbers that are generated by recursive and deterministic algorithms. Therefore, the information seems to be originated randomly and follows a required distribution. Attempts of obtaining random numbers by non-deterministic processes, like the noise of electronic tubes, failed since the distribution of values obtained have tendencies, which are not desirable for the purposes of a stochastic simulation (Sobol 1994).

For the purposes of this paper, a random/pseudo-random number is a realization (sampling) of a random variable with uniform distribution between 0 and 1 (Press et al. 1992) and it is obtained by algorithms. The most famous one is the Mersenne Twister (Matsumoto and Nishimura 1998) and it is natively implemented in most programming languages.

2.2 Latin Hypercube Sampling (LHS)

As a main idea in the Monte Carlo simulation, the parameters of the model are treated as random variables that are generated by sampling pseudo-random numbers, which are converted afterwards. So when comparing the fidelity of the distribution of the random variables to the theoretical one, the quality of the pseudo-random number generation plays a big role.

Originally, the parameters were generated without any kind of filtering on the random numbers sampled. This lead to problems of tendencies in the distribution, which caused gross inaccuracies in the results and mainly in the calculation of the uncertainties. Even for generators considered good, the tendencies issue occurs.

The approach of stratification of the domain of the random variables (Steinberg 1963) mitigated almost completely the tendency issue. By dividing the CDF's domains in equal parts (i.e. subsets with the same probability of occurrence), and then sampling once for each stratum, in each variable, a homogeneous set of data for the simulation is obtained. However, for models with a large number of variables, this stratified sampling loses in efficiency, sometimes becoming impracticable, since the number of simulations needed is the number of strata power the number of variables.

To solve this issue, the Latin Hypercube Sampling (LHS) (McKay et al. 1979) was proposed as a way to have a homogeneous and efficient sample (i.e. small number of simulations needed for convergence). The name resembles a mathematical game called Latin square, similar to a sudoku game, where in a matrix N × N must be filled with numbers or letters, with no repetition in a same line or column (Montgomery 2001). Instead of having each stratum sampled for each variable, each stratum of each variable will be used only once. Therefore, the number of simulations will no longer depend on the number of variables, being simply equal to the number of strata.

Figure 2 exemplifies and compares the Random, Stratified and Latin Hypercube sampling for a model with two variables with normal PDF. In the random sampling, although the distribution is somewhat obeyed, it is needed many samples to have a meaningful result, besides the undesirable presence of asymmetry, which aggregates tendencies to the simulation. Stratified sampling helps the result being meaningful and homogeneous with less samples, compared to the previous one; however, it is not practical for problems with too much variables. Latin Hypercube Sampling helps to generate representative results by using even less samples, being the only sampling method among these applicable to complex models, as the one employed in this paper.

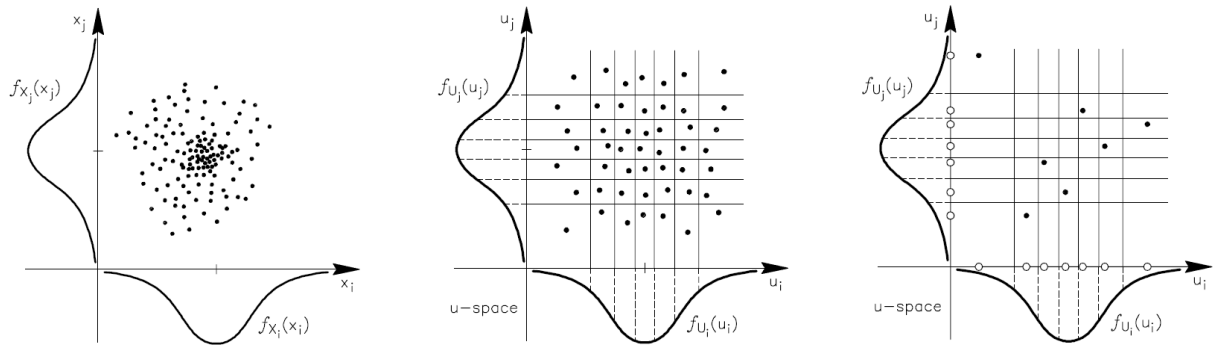

Figure 2. Random, Stratified, and Latin Hypercube Sampling. Adapted from: Hurtado and Barbat (1998)

3. MATHEMATICAL MODELLING

In order to evaluate a transient problem, the surge and swab problem of a drilling fluid was selected. The drilling pipe is inserted in the well with a constant speed. Then the fluid is projected to the bottom of the well and the pressure is increased throughout the annular space.

The mathematical modeling is divided into two parts: the transient model and the Monte Carlo – LHS method, where the uncertainties of the parameters are processed before being applied to the start-up flow model. The results are treated after all the simulations are done, as explained in the section above.

3.1 Assumptions adopted

The problem is considered: (a) one-dimensional, i.e., the pressure is a function of the axial coordinate, z; (b) transient; (c) the fluid model employed is the Bingham model; (d) the flow only occurs at the annular space between the drilling column and the well; (e) the flow is considered isothermal; (f) the flow is weakly compressible; (g) the acceleration of the drill pipe is instantaneous.

3.2 Start-up flow model

The fluid motion is governed by the mass conservation equation and the momentum equations. After applying the assumptions, for an annular pipe, the equations take the form of Eq. (7):

$$\begin{cases} \dfrac{\partial \rho}{\partial t} + \dfrac{\partial}{\partial z}\left(\rho v_z\right) = 0 \\ \dfrac{\partial \rho v_z}{\partial t} + v_z \dfrac{\partial \rho v_z}{\partial z} = -\dfrac{\partial P}{\partial z} - \dfrac{4\left(D_1\tau_1 + D_2\tau_2\right)}{D_2^2 - D_1^2} + \rho g \sin\left(\beta\right) \end{cases} \tag{7}$$

Where ρ is the density, t is the time, z is the axial position, v_z is the axial velocity, P is the pressure, D_1 is the internal diameter, D_2 is the external diameter, τ_1, τ_2 are the shear stresses at the internal and external walls, respectively, g is the gravity force, and β is the angle with horizontal (in this case, as the well is vertical, $\beta = 90°$).

The equation of state deals with the isothermal compressibility of the fluid. It is shown in Eq. (8).

$$\alpha = \frac{1}{\rho}\frac{\partial \rho}{\partial P}\bigg|_T \tag{8}$$

Where α is the compressibility, and T is the absolute temperature.

To couple the whole system of equations, it is employed the fluid's constitutive equation. In order to model the drilling fluid, it is needed to take into account its non-newtonian features. This way, the mud is modeled as a Bingham fluid. This model states that the material has a yield stress. If the stress in the fluid is bigger than the yield stress, the flow occurs. If not, the material behaves as a hookean solid. The fluid's equation is taken into account in the form of the Fanning friction factor (Eq.(9)):

$$\frac{4\left(D_1\tau_1 + D_2\tau_2\right)}{D_2^2 - D_1^2} = \frac{2 f \rho V^2}{D_2 - D_1} \tag{9}$$

Where f is the Fanning friction factor, and V is the mean velocity. The friction factor, for an annular pipe, is defined by the Eq. (10):

$$f_A = \frac{16}{\mathrm{Re}_{z,t}}\frac{\zeta}{\gamma} \tag{10}$$

In order to define the parameters of the equations, it is necessary to define some non-dimensional parameters: the Reynolds number, the Hedstron number and the bingham number (Eq. (11)):

$$\begin{aligned} \mathrm{Re}_{z,t} &= \frac{\rho_0 V_R D_h}{\eta} \\ He &= \frac{\rho \tau_y D_h^2}{\eta^2} \end{aligned} \tag{11}$$

In Eq. (10), ζ stands for a geometric parameter for the annular space, and γ is the conductance of the Bingham fluid. Those are defined by Eq. (12) and Eq. , respectively:

$$\zeta = \frac{\left(D_2 - D_1\right)^2}{D_2^2 + D_1^2 + \left[\left(D_2^2 - D_1^2\right)/\ln\left(D_2/D_1\right)\right]} \tag{12}$$

$$\gamma = 1 - \frac{\gamma He_{z,t}}{8\mathrm{Re}_{z,t}} + \frac{1}{2}\left(\frac{\gamma He_{z,t}}{12\mathrm{Re}_{z,t}}\right)^3 \tag{13}$$

3.3 Geometry

The geometry employed in this problem is a simplification based on a real oil well, with its dimensions provided by PETROBRAS. The simplified version is composed by four sections of annular space: (a) The upper section represents the drilling riser, which is a pipeline used to guide and protect the drilling column; (b) The next section is the main pipeline, built around the column; (c) Finally, the last two sections are the open part of the well. Figure [x] brings the geometry employed in the simulation, while Table [y] shows the diameters and length of all sections for the geometry.

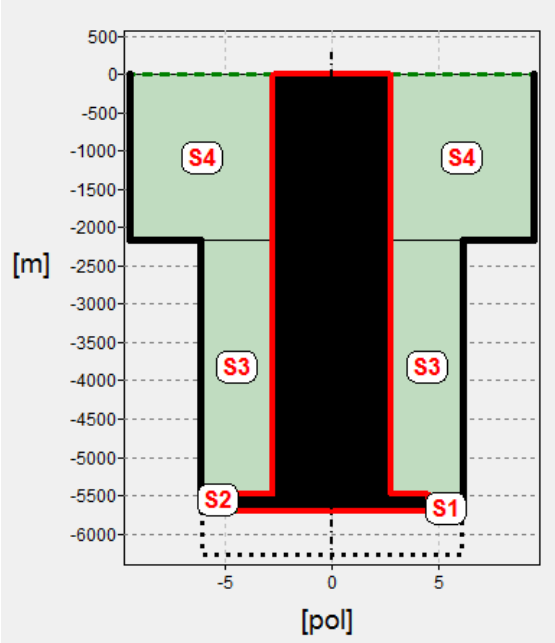

Figure 3 - Well geometry

3.4 Boundary and initial conditions

In order to solve the system presented above, it is required a set of boundary and initial conditions. Boundary conditions are related to the geometry of the problem. In the present problem, the condition employed is a constant null pressure at the open surface of column and annular space.

Since the problem is transient, it also needs initial conditions. Although these conditions can be defined for any specified time, in practical situations they are defined for the first value of time ($t = 0$). For the present problem, the initial conditions can be derived by stating that the pressure applied is the hydrostatic pressure ($\partial P/\partial z\big|_{t=0} = g\rho\big|_{t=0}$). This way, the velocity field is $\overline{V}\left(z, t=0\right) = 0$. Therefore, the initial density and pressure varies with the fluid weight and with the axial position, as shown by Eq. (14) and (15):

$$\rho\left(z, t=0\right) = \rho_0\left(1 - g\rho_0\alpha z\sin\left(\beta\right)\right)^{-1} \tag{14}$$

$$P\left(z, t=0\right) = \frac{1}{\alpha}\ln\left(1 - g\rho_0\alpha z\sin\left(\beta\right)\right) \tag{15}$$

3.5 Numerical solution

The system of governing equations is solved by an implementation of the method of characteristics. This method is typically applied to solve hyperbolic differential equations. The method simplifies the equations, converting them to a family of ordinary differential equations, making it possible to solve them by integrating from an initial condition.

3.6 Monte Carlo – LHS modelling

The Monte Carlo method begins by defining the nominal value and its uncertainties for each parameter, along with the number of strata (consequently, the number of simulations). Then the strata of each variable are numbered with indexes and the partnering process takes place (e.g. simulation 1: third stratum of first variable, eighth stratum of second variable, and so on). For each variable, each stratum appears only once.

Having all the indexes combinations, the sampling process begins. For each individual simulation, a random number is called for each variable and adapted to belong to the required stratum of its domain. This adapted number is used as an input to the inverse of the CDF, to obtain a sample of the parameter.

A set of samples (one per variable) is used as the input for the start-up flow model. Its equations are solved iteratively, the same way as a regular numerical simulation. This repeats a predefined number of times (equal to the number of strata chosen). At the end of each simulation, the interest value will be stored.

When all the simulations are finalized, the mean value is given by Eq. (16) and the uncertainty by Eq. (17), as the sample standard deviation.

$$\bar{P} = \frac{1}{N}\sum_{i=1}^{N} P_i \tag{16}$$

$$\sigma_P = \sqrt{\frac{1}{N-1}\left[\sum_{i=1}^{N} P_i^2 - \frac{1}{N}\left(\sum_{i=1}^{N} P_i\right)^2\right]} \tag{17}$$

where N is the number of simulations and P is the desired pressure value.

3.7 Uncertainties considerations

Uncertainties appear in all measurements of physical quantities. Its magnitude depends on the way of measurement, on the kind of the quantity, among others. When the measured values are applied to a mathematical model, each quantity, in the form of a parameter of the model, exercises some influence on the result. For the uncertainty quantification approach, the magnitude of the uncertainties also has considerable influence.

This way, it is important to know which variables of the equations worth being modeled as having uncertainties, by way of knowing the magnitude of the uncertainties and its influence on the equations. In a first attempt, three parameters were modeled as having uncertainties: the yield stress, the dynamic viscosity, and the column velocity.

4. RESULTS

4.1 Validation – Grid and convergence tests

In the beginning of a numerical simulation, it is recommended to perform a grid test to see which is the coarser grid that satisfies the requirements of the problem. In this paper, the axial grid was initially set to 20 control volumes, and then, consecutively doubled. Table 1 presents the results for the pressure peak. The convergence criteria is defined as: when the percentage difference between two consecutive tests is less than 1%. This way, the grid selected was 320 control volumes.

Similarly to a conventional grid test, it is necessary to run a convergence test for the MC simulation. This test aims to know the minimum number of simulations required for the mean pressures and its standard deviation values to stabilize. The convergence criteria is the same as the one employed to the grid test.

Table 2 shows the results of the convergence test, applied for the mean value of the peak pressure and its uncertainty. Based on this test, the number of simulations chosen was 160.

Table 1 - Grid test

Grid	t_ peak [s]	Peak pressure [psi]	% t	% P
20	49.73	211.60	17.11%	17.62%
40	41.23	174.32	13.49%	14.20%
80	35.67	149.57	-1.38%	0.09%
160	36.16	149.43	0.68%	1.45%
320	35.91	147.26	0.23%	0.66%
640	35.83	146.28	0.86%	-0.34%
1280	35.52	146.78	0.32%	0.18%
2560	35.41	146.52	0.09%	0.09%
5120	35.38	146.39		

Table 2 - Convergence test

				Percentage difference	
N_sim	Peak time [s]	Mean pressure [psi]	Uncertainty [psi]	% avg	% unc.
2	42.7817	147.2450	4.4999	-2.86%	68.26%
5	42.2909	143.1559	14.1785	-0.17%	31.47%
10	43.4361	142.9140	20.6898	-1.78%	8.06%
20	43.0271	140.4210	22.5036	0.73%	-15.74%
40	42.6999	141.4519	19.4430	1.01%	4.42%
80	42.9453	142.8941	20.3412	-0.48%	-5.23%
160	42.3727	142.2106	19.3298	0.04%	0.76%
320	42.8635	142.2727	19.4777	-0.04%	-1.20%
640	42.6181	142.2185	19.2474	-0.12%	-0.95%
1280	42.6181	142.0410	19.0660	0.03%	0.22%
2560	42.6181	142.0817	19.1086	0.06%	0.04%
5120	42.6181	142.1643	19.1169	-0.05%	-0.35%
10240	42.6181	142.0927	19.0507		

4.2 Case studied

For the case proposed, the parameters of the simulations were defined by PETROBRAS: The density was 9.9 ppg and the compressibility was $4.4444*10^{9}$ Pa^{-1}.The properties of the fluid were obtained by adjusting from the measures by FANN, shown in Table 3, alongside with the parameters at Table 4. The uncertainties were all set to 20% of the base value for each parameter.

Table 3 - Fluid curve

Velocity [rpm]	Deflection
600	57
300	38
200	30
100	21
6	13
3	12

Table 4 - Fluid properties

Dynamic viscosity [cP]	14.16625
Yield stress [lb/100 ft^2]	22.62439

Figure 4 shows the pressure in the bottom of the well as a function of time, when there is no uncertainties acting. Starting from $t = 0$, it is noticed an almost linear pressure increase, followed by some pressure peaks, with its magnitude being damped until the steady state is reached.

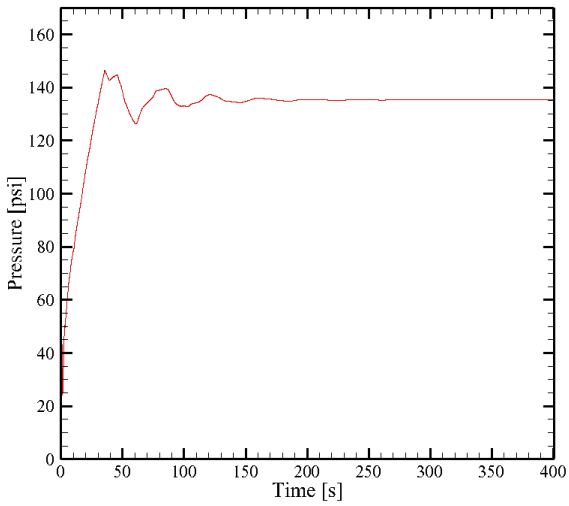

Figure 4 - Pressure x time, without uncertainties

4.3 Uncertainty effects analysis

The MCM was then applied to the simulation. Figure 5 brings the evolution of pressure, along with the correspondent uncertainty at each time step. The red curve stands for the mean pressure, the green curve is the mean pressure plus the uncertainty, and the blue one is the mean pressure minus the uncertainty.

Although the present simulation is not related at all with any kind of linearity, the uncertainties follow the mean value curve somewhat closely. Its effects are slightly bigger in the peaks and the transient part of the simulation, and smaller in the steady state region.

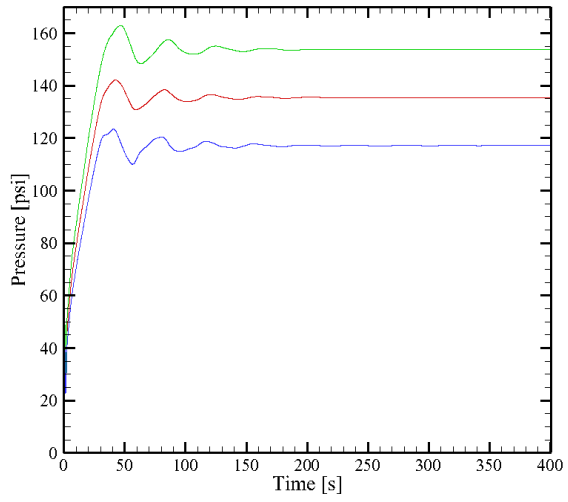

Figure 5 - Pressure x time, with uncertainties

To see the influence of the uncertainties for each variable, the MC simulation can be performed applying them in just one parameter at a time, keeping the other ones as constants. Figure 6, Figure 7 and Figure 8 shows the pressure as a function of time when the yield stress, column velocity, and viscosity, respectively, has uncertainties.

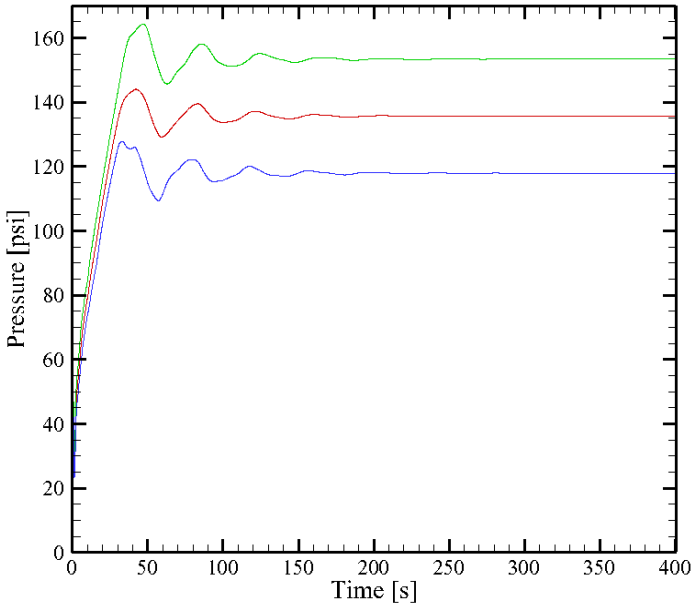

Figure 6 - P x t - Uncertainties in yield stress

As it is seen in Figure 6, the yield stress seems to account for the majority of the uncertainties. In fact, as this parameter has influence in the pressure from which the material flows, its effects are carried to the rest of the simulation, being the major source of uncertainty for the steady state.

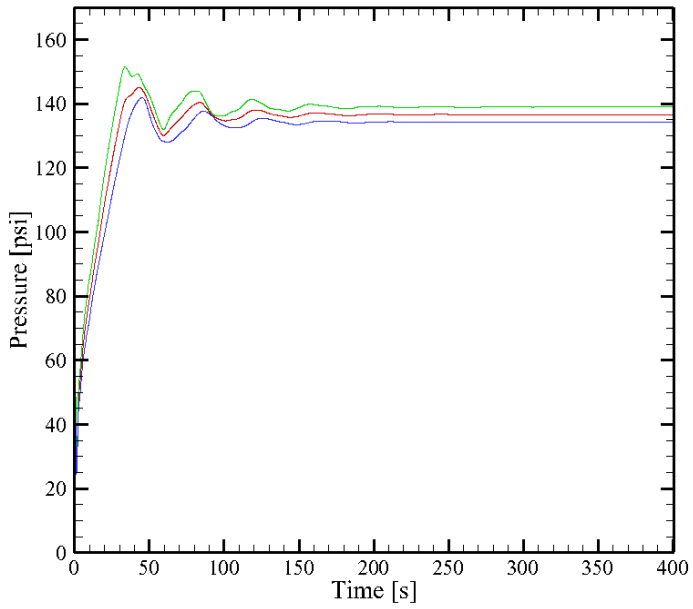

Figure 7 - P x t - Uncertainties in the column velocity

Figure 7 brings the evolution of pressure when there are uncertainties in the column velocity. On the contrary of what was shown in Figure 6, the transient region primarily governs the uncertainties. The slopes of the blue and green curves on the graph shows it. This is explained by the fact that this parameter brings the transient feature to the problem. For the steady part, its influence is smaller.

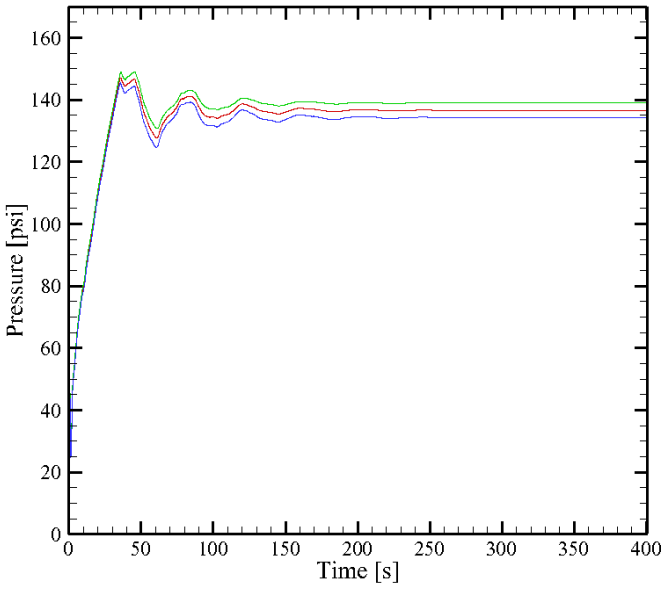

Figure 8 - P x t - Uncertainties in the viscosity

The viscosity is, by far, the parameter with the smallest influence, among the ones tested in this case study. As seen in Figure 8, the viscosity has negligible influence in the beginning of the pressure evolution. It is explained by the fact that the fluid does not flow until the yield stress is achieved. This way, this parameter only appear when the pressure peaks occurs, still with smaller influence, compared to the yield stress.

4.4 Relative uncertainties analysis

For a more quantitative analysis, it is interesting to evaluate the evolution of the relative uncertainty. It is obtained by dividing the magnitude of the uncertainty by the mean pressure, for all time steps. Similarly to what was made in section 4.3, the relative uncertainty was plotted for the four situations: All three parameters with uncertainties, and each one individually.

Figure 9 is the graph of relative uncertainty as a function of time. After $t \cong 40s$, the yield stress has the biggest contribution to the uncertainties, by a large margin. At the transient region, yield stress and column velocity share the influence on the uncertainties, having the latter a slightly bigger magnitude. In the steady region, viscosity and velocity have low contributions, with the viscosity uncertainties following the peaks of yield stress, while velocity peaks follows the valleys of yield stress.

It is also noted that the biggest values of uncertainty are present around $t \cong 50s$, in the first pressure peak. It is reasonable, since peaks in functions are inflection points, or even singularity points, where the behavior is ruled by abrupt changes and its derivatives sometimes diverges. Then, it is feasible to state that uncertainty propagation is stronger in these cases.

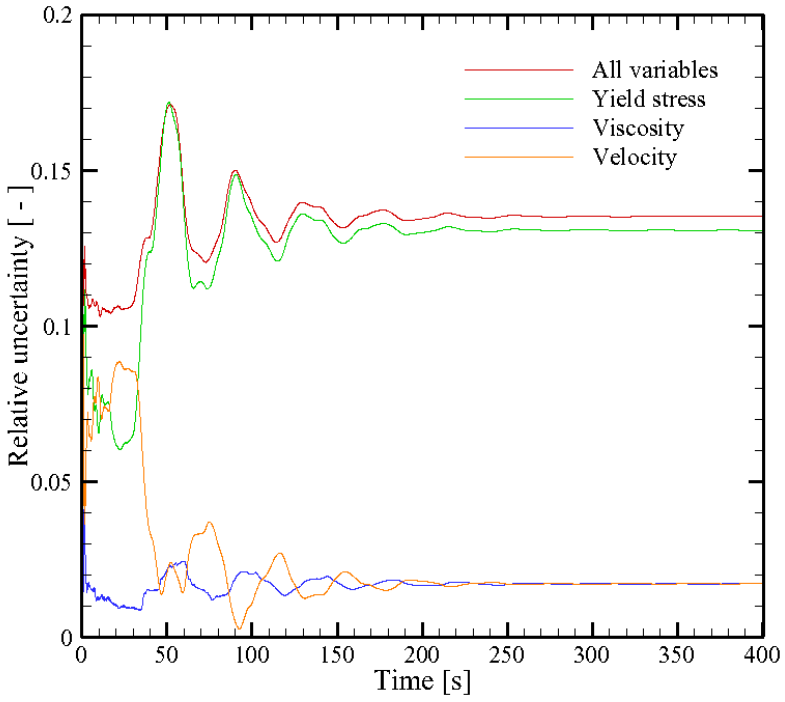

Figure 9 - Relative uncertainty x time

5. FINAL REMARKS

This paper intends to assess the uncertainties on the transient problem of surge and swab. This is going to be done by a statistical approach called Monte Carlo method (MCM). Among other stochastic methods of evaluating uncertainties (such as polynomial chaos expansion (Banek 1999), metamodeling (Zhang et al. 2013), Bayesian inference (Kennedy and O'Hagan 2001), fuzzy systems (Xiao and Cai 1997), etc.), MCM was chosen due to its simpler implementation and a bigger bibliography available.

The surge and swab problem consists in the movement of the drilling column inside of the well. There are numerous parameters to be controlled in this process, such as the local pressures along the well, the flow rate of the drilling mud, the column velocity, the properties of the mud, etc. For this implementation, the goal was to evaluate the pressure over time, considering that three variables had uncertainties: column velocity, the yield stress and viscosity of the drilling fluid.

By entering with an input of 20% of uncertainty, it turned into 13% in the result. The reason for this "shrinking" is that other parameters have more importance in the composition of the uncertainty. However, it would not be reasonable to set to 20% of uncertainty parameters such as diameters. This way, it becomes harder to compare the influence of each variable.

Among the parameters analyzed, the yield stress was responsible for the majority of the uncertainties, mainly in the steady region. The column velocity showed more influence in the transient area (with similar contribution as the yield stress). The viscosity did not show relevance to the composition of uncertainty. The bigger values of uncertainty appeared near the pressure peaks, a transient region of the curve strongly influenced by the yield stress.

The methodology approached here finds direct application in oil production platforms and process planning, since the implementation is enough general to accept the inputs as needed and takes small computational time. This way, it is a good tool to predict pressure fluctuations on the drilling maneuver.

6. ACKNOWLEDGEMENTS

The authors acknowledge the financial support of PETROBRAS S/A, ANP (Brazilian National Oil Agency), UTFPR (Federal University of Technology - Paraná) and CNPq (The Brazilian Council for Scientific and Technological Development).

7. REFERENCES

Banek T (1999) Chaos expansion for the solutions of stochastic differential equations. Syst Control Lett 36:351–358.
Bauer WF (1958) The monte carlo. SIAM J Appl Math 6:438–451.
Beasley JD, Springer SG, Moro B (2003) An algorithm for computing the inverse normal cumulative distribution function.
Bergant A, Simpson AR, Tijsseling AS (2006) Water hammer with column separation: A historical review. J Fluids Struct 22:135–171.
Caenn R, Darley HCH, Gray GR (2011) Composition and Properties of Drilling and Completion Fluids.
Cunha A, Nasser R, Sampaio R, Lopes H, Breitman K (2014) Uncertainty quantification through the Monte Carlo method in a cloud computing setting. Comput Phys Commun 185:1355–1363.
Galves LV (2013) Impacto na Solubilidade de Gás na Detecção de Kicks em Fluidos de Perfuração de Base N-Parafina.
Ghidaoui MS, Kolyshkin AA (2001) Stability Analysis of Velocity Profiles in Water-Hammer Flows. J Hydraul Eng 127:499–512.
Ghidaoui MS, Zhao M, McInnis DA, Axworthy DH (2005) A Review of Water Hammer Theory and Practice. Appl Mech Rev 58:49.
Hurtado JE, Barbat AH (1998) Monte Carlo Techniques in Computational Stochastic Mechanics. 5:3–29.
Kalos MH, Whitlock PA (2008) Monte Carlo Methods.
Kennedy MC, O'Hagan A (2001) Bayesian calibration of computer models. J R Stat Soc Ser B (Statistical Methodol 63:425–464.
Lummus JL, Azar JJ (1986) Drilling fluids optimization: a practical field approach.
Majd A, Ahmadi A, Keramat A (2016) Investigation of Non-Newtonian Fluid Effects during Transient Flows in a Pipeline. Strojniški Vestn - J Mech Eng 62:105–115.
Martínez PAM (2009) Análisis y métodos de emsambles.
Matsumoto M, Nishimura T (1998) Mersenne Twister : A 623-dimensionally equidistributed uniform pseudorandom number generator. Discrete Math 26.
McKay MD, Beckman RJ, Conover WJ (1979) Comparison of Three Methods for Selecting Values of Input Variables in the Analysis of Output from a Computer Code. 21:239–245.
Metropolis N, Ulam S (1949) The Monte Carlo Method. 46:147–190.
Montgomery DC (2001) Design and Analysis of Experiments. 286.
Morais JM De (2013) Petróleo em Águas Profundas - Uma história tecnológica da PETROBRAS na exploração e produção offshore.
Oliveira GM, Franco AT, Negrão COR (2015) Mathematical Model for Viscoplastic Fluid Hammer. J Fluids Eng 138:11301.
Oliveira GM, Negrão COR, Franco AT (2012) Pressure transmission in Bingham fluids compressed within a closed pipe. J Nonnewton Fluid Mech 169–170:121–125.
Oliveira GM de, Franco AT, Negrão COR, Martins AL, Silva RA (2013) Modeling and validation of pressure propagation in drilling fluids pumped into a closed well. J Pet Sci Eng 103:61–71.
Press WH, Teukolski SA, Vetterling WK, Flannery BP (1992) Numerical recipes in Fortran 77.
Rubinstein RY (1991) Simulation and Monte-Carlo method.
Santos OLA (2006) Segurança de Poços em Lâminas de Água Ultraprofundas.
Sobol IM (1994) A Primer for the Monte Carlo Method. 102.
Steinberg HA (1963) Generalized Quota Sampling. Nucl Sci Eng 15:142–145.
Streeter VL, Lai C (1962) Water-hammer analysis including fluid friction. J Hydraul Div 88:79–112.
Tazraei P, Riasi A (2015) Quasi-Two-Dimensional Numerical Analysis of Fast Transient Flows Considering Non-Newtonian Effects. J Fluids Eng 138:11203.
Tazraei P, Riasi A, Takabi B (2015) The influence of the non-Newtonian properties of blood on blood-hammer through the posterior cerebral artery. Math Biosci 264:119–127.
Thomas JE (2001) Fundamentos de engenharia de petróleo.
Triola M (2017) Elementary Statistics.
Wahba EM (2013) Non-Newtonian fluid hammer in elastic circular pipes: Shear-thinning and shear-thickening effects. J Nonnewton Fluid Mech 198:24–30.
Wahba EM (2006) Runge–Kutta time-stepping schemes with TVD central differencing for the water hammer equations. Int J Numer Methods Fluids 52:571–590.
Wylie EB, Streeter VL, Suo L (1993) Fluid transients in systems.
Xiao XX, Cai Z (1997) Quantification of uncertainty and training of fuzzy logic systems. IEEE Int Conf Intelllient Process Syst 312–316.
Yang S, Wu D, Lai Z, Du T (2017) Three-dimensional computational fluid dynamics simulation of valve-induced water hammer. Proc Inst Mech Eng Part C J Mech Eng Sci 231:2263–2274.
Zhang S, Zhu P, Chen W, Arendt P (2013) Concurrent treatment of parametric uncertainty and metamodeling uncertainty in robust design. Struct Multidiscip Optim 47:63–76.

Zhao M, Ghidaoui MS (2003) Efficient Quasi-Two-Dimensional Model for Water Hammer Problems. J Hydraul Eng 129:1007–1013.

8. RESPONSIBILITY NOTICE

The authors are the only responsible for the printed material included in this paper.